International Journal of Electrical, Electronic and Communication Sciences
ISSN: 2517-9438
Vol:5, No:12, 2011

Investigation of I/Q Imbalance in Coherent Optical OFDM System

R. S. Fyath and Mustafa A. B. Al-Qadi

***Abstract*—**The inphase/quadrature (I/Q) amplitude and phase imbalance effects are studied in coherent optical orthogonal frequency division multiplexing (CO-OFDM) systems. An analytical model for the I/Q imbalance is developed and supported by simulation results. The results indicate that the I/Q imbalance degrades the BER performance considerably.

***Keywords*—**Coherent detection, I/Q imbalance, OFDM, optical communications

I. Introduction

THE trend toward the reconfigurable optical networks with high transport speeds poses some challenges to the network design. For example, the signal has become extremely sensitive to the chromatic dispersion (CD), polarization mode dispersion (PMD), filtering effects of add/drop multiplexers, and the imperfection of the optoelectronic components [1]. Therefore, it is mandatory that the per-channel optical dispersion compensation is used. Furthermore, to support long-haul transmission in the range of 1000 km, even the best fiber link requires PMD compensation for high transmission speeds. Optical PMD compensators are bulky, lossy, and expensive. As such, an adaptive optical transmission system for an agile and reconfigurable optical network is essential to support high capacity and ever evolving user demands. Optical orthogonal frequency division multiplexing (O-OFDM) systems have recently been proposed to satisfy all the above-mentioned requirements for the flexible optical transmission networks which are needed for today and future applications [2], [3].

Recently, there is increasing interest in coherent optical OFDM (CO-OFDM) system which is a promising technology for long-haul and high-speed optical transmission systems. It combines the advantages of both *coherent detection* and *OFDM* scheme to improve power and spectral efficiency, and to facilitate flexible impairment compensation using digital signal processing (DSP) [4], [5]. This gives the system its superior performance that makes it the best candidate to the next generation of optical transmission systems.

A simplified analysis of OFDM scheme assumes linearity among all the system stages between the transmitter inverse fast Fourier transform (IFFT) and receiver FFT. The nonlinearity or imbalance in signal components in any part of the system causes performance degradation due to intersymbol interference (ISI) and/or intercarrier interference (ICI) effects. One of these nonlinearities that can affect the performance is the mismatch between the inphase (I) and quadrature phase (Q) components of the complex OFDM signal, the "I/Q *imbalance*" [6], [7]. This imbalance can be in the phase and/or the amplitude of the I and Q components of the OFDM signal.

Many parts of the system can contribute in inducing the imbalance between the I and Q parts of the optical OFDM signal. The imbalance can be induced by the RF and/or the optical components of the system. For example, the imbalance can be produced by the imperfection or bias deviation in the digital-to-analog convertors (DACs)/ analog-to-digital convertors (ADCs), the imperfection in the optical splitters in the transmitter or receiver sides, the difference in the insertion loss value between the two Mach-Zehnder modulators (MZMs) of the I/Q optical modulator at the transmitter [8], and the imperfection or imbalance in splitting the power in the optical hybrid of the CO-OFDM receiver [9]. The I/Q imbalance induced at the transmitter side causes image interference from the subcarriers symmetrical with respect to the transmitter laser, and similarly receiver-side I/Q imbalance causes image interference among symmetrical subcarriers with respect to the local oscillator. As a result, each constellation point is deformed and spread due to random interference from symmetrically opposite subcarrier. This ICI is one of the challenges against using higher-order constellations to achieve high spectral efficiency in CO-OFDM systems.

In this paper, the I/Q imbalance and its effects on the performance of CO-OFDM system are studied and explained, and a mathematical model including amplitude and phase imbalance is developed. Simulation results for I/Q imbalance are presented using "OptiSystem Ver. 9" software package and the results are used to elucidate the influence of imbalance on system performance and to determine the relation between the formulated imbalance parameters and transmission bit error rate (BER).

II. Coherent Optical OFDM

A generic O-OFDM system is depicted in Fig. 1. It consists of five basic functional blocks: (i) RF OFDM transmitter, (ii) RF-to-optical (RTO) up-converter, (iii) optical channel, (iv) optical-to-RF (OTR) down-converter, and (v) RF OFDM receiver.

Optical OFDM is a special form of optical MCM techniques, employing overlapped orthogonal signal set, with an increased spectral efficiency.

R. S. Fyath is with the Department of Electronic and Communications Engineering, Al-Nahrain University, Baghdad, Iraq. (phone: 00964(0)7901340801; e-mail: rsfyath@yahoo.com).

Mustafa A. B. AL-Qadi is with the Department of Electronic and Communications Engineering, Al-Nahrain University, Baghdad, Iraq. (phone: 00964(0)7901567162; e-mail: mustafaelec20052@yahoo.com).

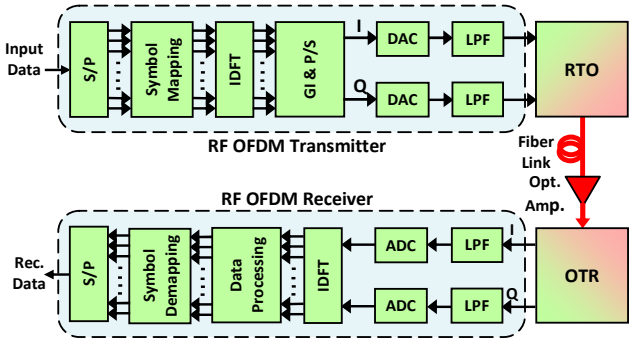

Fig. 1 Schematic of a generic O-OFDM communication system

As shown in Fig. 1, the input digital data to the RF OFDM transmitter is serial-to-parallel converted into blocks of bits consisting of N_{sc} information symbols; each may comprise multiple bits for m-ary coding. These information symbols are mapped into two-dimensional complex signal C_{ki}, where C_{ki} represents the mapped information symbol to be modulated on the kth subcarrier at the ith instant. The inverse discrete Fourier transform (IDFT) is applied to the ith set of C_k symbols to produce the time-domain samples of the ith "*OFDM symbol*", utilizing the computationally-efficient FFT algorithm. A guard interval is then inserted to avoid channel dispersion. The resulting baseband OFDM signal $s_B(t)$ can be expressed as [10]

$$s_B(t) = \sum_{i=-\infty}^{\infty} \sum_{k=-N_{sc}/2+1}^{N_{sc}/2} C_{ki}\Pi(t - iT_s)\exp\left(j2\pi f_k(t - iT_s)\right) \quad (1a)$$

$$f_k = \frac{k-1}{T_s}, \quad (1b)$$

$$\Pi(t) = \begin{cases} 1, & (-\Delta_G < t \le t_s) \\ 0, & (t \le -\Delta_G, t > t_s) \end{cases} \quad (1c)$$

where N_{sc} is the number of OFDM subcarriers, T_s is the OFDM symbol period, f_k is the frequency of the kth subcarrier, Δ_G is the guard interval length, and t_s is the observation period during which the OFDM symbol is to be captured at the receiver, and $\Pi(t)$ is the rectangular pulse waveform of the OFDM symbol.

The digital OFDM signal is converted to analog form through DACs and filtered with low-pass filters (LPFs) to remove the unwanted alias sideband signals. The baseband OFDM signal is then either converted into an IF signal, by an I/Q modulator, and then to optical domain, or directly converted to the optical domain, depending on the system configuration [11]. At the receiver end, the baseband OFDM signal is sampled by ADCs, and demodulated by performing the discrete Fourier transform (DFT) and baseband signal processing to recover the data.

In CO-OFDM the electric field spectrum of the transmitted optical signal is a replica of the baseband RF OFDM signal, with no need for any optical carrier component to be transmitted. Instead, the carrier component needed for OTR-conversion is locally generated at the receiver.

Fig. 2 shows the conceptual diagram of a direct up/down conversion architecture for CO-OFDM systems [11], [12]. In direct RTO up conversion, the RTO is simply an optical I/Q modulator comprises two MZMs to convert the I and Q components of the baseband OFDM signal to the optical domain directly. In the direct down conversion architecture, the OTR converter uses two pairs of PD receivers and optical hybrids to perform optical to electrical I/Q detection.

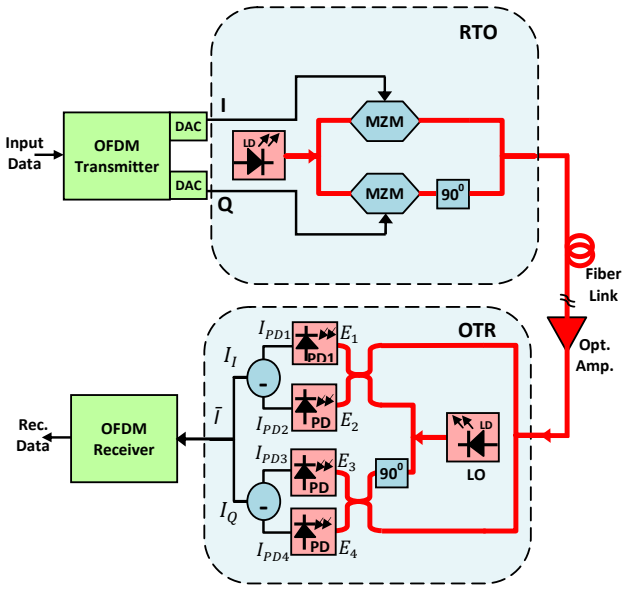

Fig. 2 Architecture of CO-OFDM system with direct up/down conversion

III. Mathematical Modeling for the I/Q Imbalance in CO-OFDM

The I/Q imbalance is modeled as amplitude and/or phase errors in the optical carrier used for modulation at the transmitter and the optical LO signal used for down conversion at the receiver. For the coherent detection scheme shown in Fig. 2, the electric field of the incoming optical signal, E_S, can be expressed as

$$E_S = E_r' + E_{ASE} \quad (2)$$

where E_{ASE} is the amplified spontaneous emission (ASE) noise introduced by the in-line optical amplifiers and E_r' is the received signal field in the absence of ASE noise. In the presence of I/Q imbalance at the transmitter side, the received signal can be expressed as

$$E_r' = E_{rr} + je^{j\emptyset_t}G_tE_{ri} \quad (3a)$$

$$= [E_{rr} - G_t sin\emptyset_t E_{ri}] + jG_t cos\emptyset_t E_{ri} \quad (3b)$$

where the I/Q imbalance is described by amplitude parameter G_t and phase parameter $\emptyset_t$. Further, E_{rr} and E_{ri} represent, respectively, the real and imaginary parts of the received signal in absence of I/Q imbalance and ASE, E_r; that is

$$E_r = E_{rr} + jE_{ri} \quad (4)$$

For perfect balance, G_t and $\emptyset_t$ tend to be one and zero, respectively, and $(3a)$ reduces to (4).

Similarly, the LO signal can be expressed as

$$E_{LO} = E'_L + E_{IN} \quad (5)$$

where E_{IN} is the intensity noise and E'_L is the LO field in the absence of intensity noise. The same fashion used in (3) can be used for E'_L to describe the imbalance parameters to form

$$E'_L = E_{Lr} + je^{j\emptyset_r} G_r E_{Li} \quad (6a)$$

$$= [E_{Lr} - (1 - a_r)sin\emptyset_r E_{Li}] + j(1 - a_r)cos\emptyset_r E_{Li} \quad (6b)$$

where G_r and $\emptyset_r$ are the amplitude and phase imbalance parameters for the receiver side, respectively. From this, the LO signal field in absence of both I/Q imbalance and intensity noise can be expressed as

$$E_L = E_{Lr} + jE_{Li} \quad (7)$$

where E_{Lr} and E_{Li} are the real and imaginary parts of E_L, respectively.

The output signals E_{1-4} of the 6-port optical hybrid are given by [13]

$$E_1 = \frac{1}{\sqrt{2}}[E_S + E_{LO}] \quad (8a)$$

$$E_2 = \frac{1}{\sqrt{2}}[E_S - E_{LO}] \quad (8b)$$

$$E_3 = \frac{1}{\sqrt{2}}[E_S - jE_{LO}] \quad (8c)$$

$$E_4 = \frac{1}{\sqrt{2}}[E_S + jE_{LO}] \quad (8d)$$

where in writing (8*a*)-(8*d*) it is assumed that the hybrid is lossless.

The corresponding photocurrents generated at the photodiodes can be found by the square rule as

$$I_{PD1} = |E_1|^2 = \frac{1}{2}[|E_S|^2 + |E_{LO}|^2 + 2\mathcal{R}e(E_S E^*_{LO})] \quad (9a)$$

$$I_{PD2} = |E_2|^2 = \frac{1}{2}[|E_S|^2 + |E_{LO}|^2 - 2\mathcal{R}e(E_S E^*_{LO})] \quad (9b)$$

$$I_{PD3} = |E_3|^2 = \frac{1}{2}[|E_S|^2 + |E_{LO}|^2 + 2Im(E_S E^*_{LO})] \quad (9c)$$

$$I_{PD4} = |E_4|^2 = \frac{1}{2}[|E_S|^2 + |E_{LO}|^2 - 2Im(E_S E^*_{LO})] \quad (9d)$$

where $\mathcal{R}e(\cdot)$ and $Im(\cdot)$ represent the real and imaginary parts of the argument, respectively; and the responsivity is assumed to have unity value for all photodiodes for simplicity. Further [13]

$$|E_S|^2 = |E'_r|^2 + |E_{ASE}|^2 + 2\mathcal{R}e(E'_r E^*_{ASE}) \quad (10a)$$

$$|E_{LO}|^2 = I_{LO}(1 + I_{RIN}) \quad (10b)$$

where I_{LO} and I_{RIN} are the average power and relative intensity noise (RIN) of the local laser, respectively.

The real and imaginary parts of the OFDM signal represented by the photocurrents I and Q, respectively, can be obtained by the first and second pairs of balanced detectors; that is

$$I_I = I_{PD1} - I_{PD2} = I_{I_o} + \Delta I_I \quad (11)$$

where I_{I_o} represents the OFDM I-component in the absence of I/Q imbalance and ΔI_I represents the change in the I component photocurrent introduced by the presence of I/Q imbalance. These can be expressed as

$$I_{I_o} = 2(E_{rr}E_{Lr} + E_{ri}E_{Li}) = 2\mathcal{R}e(E_r E^*_L) \quad (12)$$

and

$$\Delta I_I = 2([G_t\, G_r \cos(\emptyset_t - \emptyset_r) - 1]E_{ri}E_{Li} - [G_r sin\emptyset_r E_{rr}E_{Li} + G_t sin\emptyset_t E_{ri}E_{Lr}]) \quad (13)$$

For a perfectly balanced system, (i.e., $G_t = G_r = 1$, $\emptyset_t = \emptyset_r = 0$), ΔI_I reduces to zero. It is worth to note that the balance detection suppresses the noise terms described in (10*a*) and (10*b*).

Similarly, the photocurrent representing the OFDM Q-component can be expressed as

$$I_Q = I_{PD3} - I_{PD4} = I_{Q_o} + \Delta I_Q \quad (14)$$

where

$$I_{Q_o} = 2(E_{ri}E_{Lr} + E_{rr}E_{Li}) = 2Im(E_r E^*_L) \quad (15)$$

and

$$\Delta I_Q = 2([1 - G_r cos\emptyset_r]E_{rr}E_{Li} - [1 - G_t cos\emptyset_t]E_{ri} + G_t G_r sin(\emptyset_t - \emptyset_r)E_{ri}E_{Li}) \quad (16)$$

Here, I_{Q_o} represents the Q component of the OFDM signal in the absence of I/Q imbalance, which changes by ΔI_Q when the imbalance exists.

The complex OFDM signal is represented by the complex photocurrent $\bar{I}$ consisting of both I and Q components; that is

$$\bar{I} = I_I + jI_Q = \bar{I}_o + \Delta\bar{I} \quad (17)$$

where

$$\bar{I}_o = 2[E_{rr}E_{Lr} + E_{ri}E_{Li} + j(E_{ri}E_{Lr} - E_{rr}E_{Li})] = 2(E_r . E^*_L) \quad (18)$$

$\bar{I}_o$ is the complex photocurrent at perfect I/Q balance condition and it is in essence a linear replica of the incoming complex signal that is frequency down-converted by a LO frequency.

It is worth to examine (13) and (16) when only phase imbalance exists (i.e., $G_t = G_r = 1$). In this case ΔI_I and ΔI_Q read

$$\Delta I_I = 2([\cos(\emptyset_t - \emptyset_r) - 1]E_{ri} - [sin\emptyset_r E_{rr}E_{Li} + sin\emptyset_t E_{ri}E_{Lr}]) \quad (19a)$$

$$\Delta I_Q = 2([1 - cos\emptyset_r]E_{rr}E_{Li} - [1 - cos\emptyset_t]E_{ri}E_{Lr} + sin(\emptyset_t - \emptyset_r)E_{ri}E_{Li}) \quad (19b)$$

Investigating (19*a*) and (19*b*) reveals that the I/Q phase imbalance induced at the transmitter cannot be compensated by introducing I/Q phase mitigation mismatch at the receiver. This is clear since ΔI_I and ΔI_Q, defined in (4.18*a*) and (4.18*b*), respectively, do not reduce to zero when $\emptyset_t = \pm\emptyset_r$.

IV. Simulation Results

The CO-OFDM system under investigation is shown in Fig. 2. The system uses direct up/down conversion method. Unless otherwise stated, the parameters values used in the simulation are listed in Table I. The system uses standard single-mode fiber with in-line Erbium-doped fiber amplifiers (EDFAs) to compensate fiber loss.

TABLE I
PARAMETERS VALUES USED IN SIMULATION

Parameter	Value
Bit rate	10 Gb/s
Central wavelength/frequency	1552.52nm /193.1 THz
Coupling ratio of transmitter and receiver X-couplers	0.5
Differential group delay	0.2 ps/km
Dispersion parameter, *D*	16.75 ps/(km-nm)
Fiber attenuation	0.2 dB/km
Gain of inline optical amplifier after each nominal span	20 dB
Linewidth of transmitter and LO LDs	150 kHz
LO optical power	0 dBm
Modulation type	QPSK
MZMs extinction ratio	60 dB
MZMs insertion loss	1 dB
MZMs switching bias voltage	4 V
Number of FFT points	1024
Number of OFDM subcariers , *Nsc*	512
Noise figure of in-line amplifiers	4 dB
Nominal fiber single-span length	100 km
Power launched to the fiber	-10 dBm
Receiver PDs dark current	10 nA
Receiver PDs responsivity	1 A/W
Receiver PDs thermal noise	1×10^{-22} W/Hz
Transmitter LD optical power	0 dBm
Transmitter optical booster gain	11 dB

The RTO up-converter (the I/Q optical modulator) is built up using an X-coupler, two Mach-Zehnder modulators, and an optical combiner. The optical signal from the laser source is applied to the 1st input port of the coupler to yield the I and Q carrier components, at the output ports, which are fed to the MZMs, as shown in Fig. 3. Lithium Niubate MZM (LiNb-MZM) with dual-drive type is used. Each MZM is driven by the positive and negative signals of one of the components of the baseband OFDM signal (I or Q) at the two inputs of modulating signal of the MZM. The output signals from the two MZMs are combined by the optical combiner to form the complex optical OFDM signal to be amplified and transmitted.

The OTR down-converter is built up using four X-couplers, a 90° phase shifter, four PIN photodetectors, and two electrical subtractors, as shown in Fig. 4. This OTR conversion network employs balanced detectors for noise cancellation.

The first coupler is used to split the incoming complex O-OFDM signal into two parts to be used for extracting the I and Q components of the OFDM separately. Similarly, the second coupler is used to split the LO signal into two parts to be mixed with the O-OFDM signal in the I and Q branches.

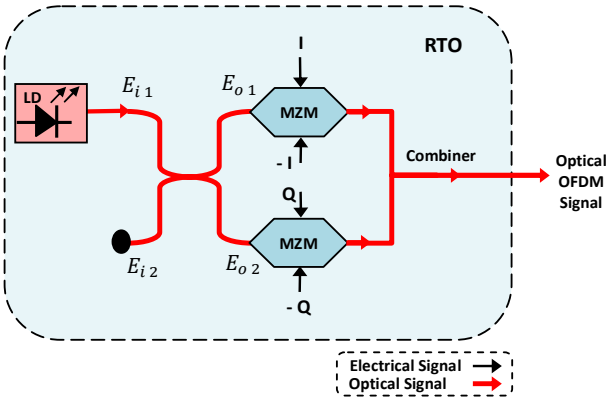

Fig. 3 Direct up-converter built for simulation

The LO signal in one of the branches is phase-shifted with 90° by the optical phase shifter to be coupled to the O-OFDM signal at the third coupler. The outputs from the third coupler are used to be fed to the PDs of the balanced detector to generate the I component of the baseband OFDM signal after subtracting the photocurrents output from the two PDs, as shown in Fig. 4. The Q component of the baseband OFDM signal is generated by the same way at the balanced detector containing the fourth coupler.

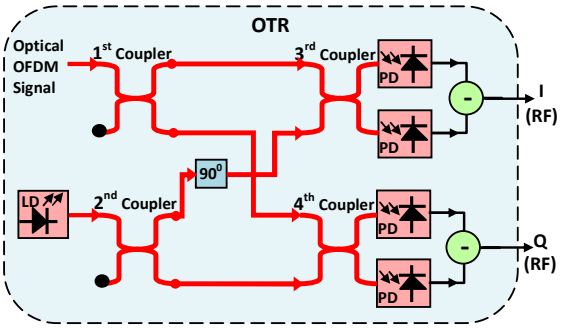

Fig. 4 Direct down-converter built for simulation

To induce an I/Q amplitude imbalance in the system, an optical gain component is used in the simulation to change the amplitude of the field of optical signal in the Q-branch of the LO signal before being fed to the optical hybrid. The scaling imbalance parameter, G_r, can then be varied in this branch to induce an amplitude imbalance between the I and Q branches of the LO signal as desired.

Fig. 5 shows the constellation diagram of the received signal with back-to-back transmission with and without applying an imbalance of (0.7) at the Q-branch of the LO signal. It can be seen that the I/Q amplitude imbalance results in spread in the constellation points due to the interference of each subcarrier with the symmetric subcarrier around the LO center frequency. Each constellation splits into many new sub-constellations which number is as many as the number of the original constellations (four in this example of QPSK).As

mentioned before, the imbalance may come from electrical or the optical components of the system. When the imbalance is induced by some electrical part, the change in the signal amplitude in one of the two branches does not affect the signal in the other branch. Whereas when the imbalance is induced by some optical component and the optical signal level is changed in one branch, the signal level in the other branch may and may not get influenced, depending on the reason of the optical amplitude imbalance. For example, if the imbalance occurs due to the difference in the insertion loss of the two (I- and Q-branch) MZMs, that is if the insertion loss of one of the MZMs is changed, the signal level at the output of the other MZM does not change. This is true since the two branches are independent. But if the imbalance is caused by some optical splitter (due to aging or thermal effects) the decrement in the signal level at one branch will correspond an increment in the signal level at the other branch. For investigating the effect of the latter case on system performance, which has more complexity, let us consider the above-mentioned scaling parameter G_r as the scaling factor for the signal level at the Q-branch of the LO signal, and denote it as G_{rQ}. And assume that the scaling parameter at the I-branch is G_{rI}.

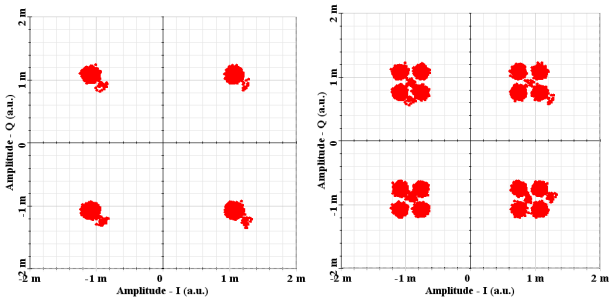

(a) (b)

Fig. 5 Constellation diagrams of the received signal with back-to-back transmission (a) without imbalance and (b) with an amplitude scaling factor of 0.7 in the Q-branch of the LO signal

Assuming that the split components in the system are lossless, the value of total output optical power from the two ports of the split device is constant regardless of the split ratio. That is

$$P_I + P_Q = constant \tag{20}$$

where P_I/P_Q represents the optical power at the I-/Q-branch. From which

$$G_{rI}{}^2 + G_{rQ}{}^2 = 2 \tag{21a}$$

or

$$G_{rI} = \sqrt{2 - G_{rQ}{}^2} \tag{21b}$$

Let us define a new imbalance parameter (B), where

$$\mathrm{B} = 1 - \frac{G_{rQ}}{G_{rI}} \tag{22}$$

This parameter has a value of zero when the powers at the two branches are equal.

Fig. 6 shows the transmission BER as a function of B for different link lengths. As expected, the system performance degrades as the imbalance parameter increases. In the absence of imbalance (B = 0), BERs of 2.3×10^{-5}, 6.1×10^{-5}, 2.3×10^{-4}, and 5.1×10^{-4} are obtained when the link lengths are 1300, 1500, 1700, and 1900 km, respectively. These values are to be compared with BERs of 8.4×10^{-5}, 2.4×10^{-4}, 4.3×10^{-4}, and 9.3×10^{-4}, respectively, when amplitude imbalance exists in the system with B = 0.2.

The constellation diagrams of the received signal for the link of 1700 km at B = 0 and B = 0.4 (G_{rQ}= 0.73, G_{rI}= 1.21) can be seen in Fig. 7.

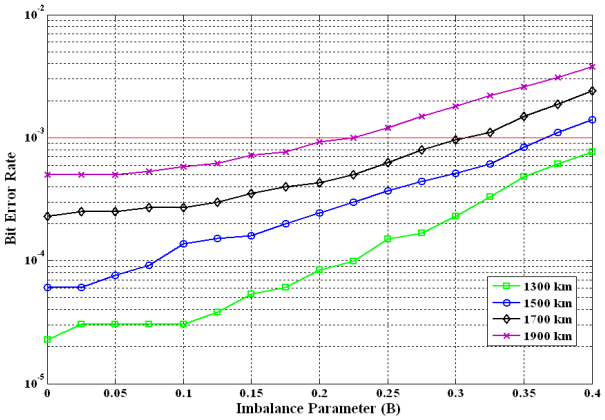

Fig. 6 BER as a function of amplitude imbalance parameter B for different link lengths

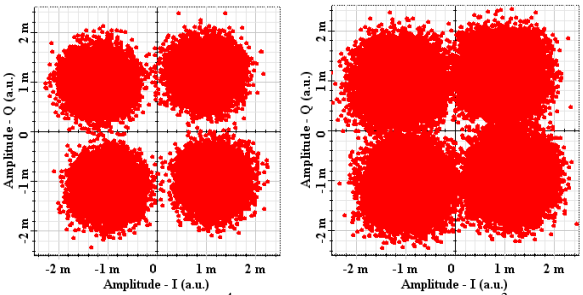

BER=2.3×10^{-4} BER=2.4×10^{-3}

(a) (b)

Fig. 7 Constellation diagrams of the received signal after 1700 km for (a) B=0 and (b) B = 0.4

The simulation is carried out further to investigate the effect of phase imbalance between the I- and Q-branches on system performance. Fig. 8 shows the BER versus the phase imbalance in the Q-branch of the optical signal of LO for different link lengths. The BER performance degrades with increasing phase imbalance. In the presence of phase imbalance of 6°, the BER increases to 6.9×10^{-5}, 1.9×10^{-4}, 5.3×10^{-4}, and 9.2×10^{-4} when the length of the link is 1300, 1500, 1700, and 1900 km, respectively.

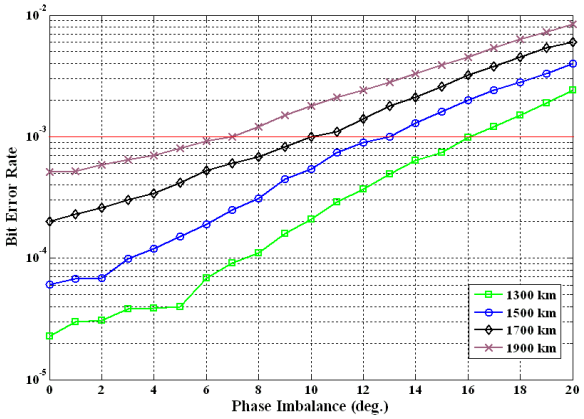

Fig. 8 BER as a function of phase imbalance for different link lengths

The effect of phase imbalance on signal constellation can be seen in Fig. 9, where the constellation diagrams for the received signal after 1700 km with different phase imbalance degrees are shown.

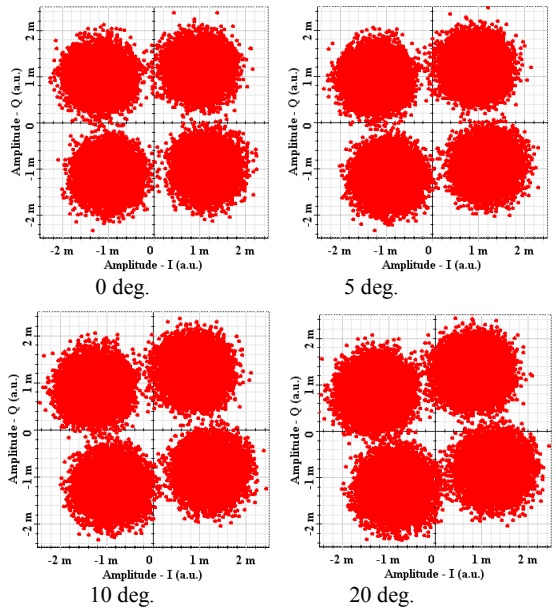

Fig. 9 Constellation diagrams after 1700 km for different values of phase imbalance

V. Conclusion

The effect of I/Q imbalance on the performance of a 10 Gb/s CO-OFDM system operating with QPSK modulation has been investigated for long-haul transmission. The results indicate that the amplitude I/Q imbalance causes spread in the received constellation points due to the interference of each subcarrier with the symmetric subcarrier around the LD/LO center frequency. Each constellation splits into many new sub-constellations, and this results in an increment in the BER. Further, The I/Q phase imbalance also degrades the BER performance of CO-OFDM considerably. For example, the BER value is 2.3×10^{-5}, 6.1×10^{-5}, 2.3×10^{-4}, and 5.1×10^{-4} with ideal balance; but in the presence of phase imbalance of 6^{o}, the BER increases to 6.9×10^{-5}, 1.9×10^{-4}, 5.3×10^{-4}, and 9.2×10^{-4} when the length of the link is 1300, 1500, 1700, and 1900 km, respectively.

References

[1] M. M.-K. Liu, "Principles and applications of optical communications," McGraw-Hill, Chicago, 1996.
[2] W. Shieh, Q. Yang, and Y. Ma, "107 Gb/s coherent optical OFDM transmission over 1000-km SSMF fiber using orthogonal band multiplexing," Optics Express, vol. 16, no. 9, pp. 6378-6386, April 2008.
[3] I. B. Djordjevic and B. Vasic, "Orthogonal frequency division multiplexing for high-speed optical transmission," Optics Express, vol. 14, no. 9, pp. 3767-3775, May 2006.
[4] A. J. Lowery, "Fiber nonlinearity mitigation in optical links that use OFDM for dispersion compensation," IEEE Photonics Technology Letters, vol. 19, no. 19, pp. 1556-1558, October 2007.
[5] B. J. C. Schmidt, A. J. Lowery, and J. Armstrong, "Experimental demonstrations of electronic dispersion compensation for long-haul transmission using direct detection optical OFDM," Journal of Lightwave Technology, vol. 26, no. 1, pp. 196-203, January 2008.
[6] A. Tarighat, R. Bagheri, A. H. Sayed, "Compensation schemes and performance analysis of IQ imbalances in OFDM receivers," IEEE Transactions on Signal Processing, vol. 53, no. 8, pp. 3257-3268, August 2005.
[7] C. F. Gu, C. L. Law, W. Wu, "Time domain IQ imbalance compensation for wideband wireless systems," IEEE Communications Letters, vol. 14, no. 6, pp. 539-541, June 2010.
[8] W.-R. Peng, B. Zhang, X, Wu, K.-M. Feng, A. E. Willner, and S. Chi, "Experimental demonstration of compensating the I/Q imbalance and bias deviation of the Mach-Zehnder modulator for an RF-tone assisted optical OFDM system," European Conference on Optical Communication (ECOC), 21-25 September, pp. 1-2, Brussels, 2008.
[9] C. S. Petrou, I. Roudas, and L. Raptis, "Impact of receiver imperfections on the performance of coherent intradyne DQPSK receivers," Conference on Lasers and Electro-Optics (CLEO), 4-9 May, pp. 1-2, San Jose, CA, 2008.
[10] W. Shieh, X. Yi, Y. Ma, and Q. Yang, "Coherent optical OFDM: has its time come [Invited]," Journal of Optical Networking, vol. 7, no. 3, pp. 234-235, March 2008.
[11] W. Shieh, H. Bao, and Y. Tang, "Coherent optical OFDM: theory and design," Optics Express, vol. 16, no. 2, pp. 841-859, January 2008.
[12] Q. Yang, W Shieh, and Y. Ma, "Bit and power loading for coherent optical OFDM," IEEE Photonics Technology Letters, vol. 20, no. 15, pp. 1305-1307, August 2008.
[13] W. Shieh and I. Djordjevic, "OFDM for optical communications," Elsevier, Amsterdam, 2010.